

Magnetic flux instabilities in superconducting niobium rings: Tuning the avalanche behavior

E. R. Nowak, O. W. Taylor, Li Liu, and H. M. Jaeger

The James Franck Institute and Department of Physics, The University of Chicago, Chicago, Illinois 60637

T. I. Selinder

Materials Science Division, Argonne National Laboratory, Argonne, Illinois 60439

(Received 11 October 1996)

We study the dynamics of superconducting vortices in Nb rings as the system is continuously driven to the depinning threshold by the slow ramping of an external magnetic field. Miniature Hall probes simultaneously detect local and global flux changes arising from vortex motion. With decreasing temperature, the dynamics evolve continuously from smooth flow to several types of avalanche behavior. In particular, we observe a crossover from broad to narrow size distributions of avalanche events which correspond to global decreases in the flux density gradient rather than local redistributions of flux. We show how this evolution can arise from the magnetothermal instability of the Bean state. [S0163-1829(97)01517-8]

Quantized vortices of magnetic flux that penetrate type-II superconductors exhibit rich dynamical behavior when driven by an external force. The motion of vortices depends crucially on the presence of pinning centers, which lead to flux gradients inside the superconductors, e.g., as described by the Bean model.¹ This nonuniform flux distribution does not correspond to an equilibrium state and under certain conditions the system can become unstable and give rise to nonlinear, collective responses such as flux jumps. In the semiclassical description, vortex motion lacks inertia and so the dynamics are overdamped. Depinning events resulting from the local competition between vortex-vortex and vortex-defect interactions in this case can remain localized and a broad distribution of jump sizes may be expected. Consequently, vortex avalanches have been thought of as a model system for experimental investigations of self-organized criticality (SOC).² SOC views the depinning threshold as a critical point, analogous to a second-order thermodynamic phase transition, and predicts power-law distributions of avalanche sizes and durations without requiring any tuning of external parameters. Simulations³ and experiments on magnetic flux penetration into superconducting tubes^{4,5} and films⁶⁻⁸ have, indeed, shown broad distributions of flux jump sizes sometimes compatible with power laws over 1–2 orders of magnitude.⁵ Other experiments, however, have found comparatively narrow size distributions centered around large breakdown events.^{9,10}

An alternative mechanism for the Bean state to become unstable is the interaction between two inherent properties of superconductors: (a) any motion of the nonsuperconducting vortex cores generates heat and (b) the critical current density falls with temperature. This produces a feedback, here called “thermal inertia,” which can reinforce the original perturbation and give rise to “catastrophic” flux jumps involving macroscopic redistributions of flux that may heat the sample temporarily into the normal state.⁹

The degree and manner in which each of these mechanisms contributes to the flux jump distributions that have been observed remains an unsettled issue. In this paper, we demonstrate that the magnetothermal properties of a type-II

superconductor lead to a whole spectrum of dynamical responses, including smooth vortex flow, broad distributions of avalanche sizes, and relaxation oscillations. We have systematically investigated the nature of the instability leading to these vortex avalanches by monitoring simultaneously the local and global motion of field-gradient driven vortices along a self-organized flux density gradient in a conventional type-II superconductor, niobium. A model for the magnetothermal stability of the vortex state can account for the observed onset of avalanche activity in the H - T plane and qualitatively explains the evolution of avalanche behavior. We do not find that the dynamical behavior at the depinning threshold represents a global attractor for the dynamics, as would be required for the applicability of SOC.

Nb rings were made from 5000-Å-thick films which were grown on $\langle 10\bar{1} \rangle$ sapphire substrates by magnetron sputtering. These films exhibited sharp superconducting transitions at a temperature $T_c = 8.9$ K, resistivities ρ (9 K) = 0.8 $\mu\Omega$ cm, and residual resistivity ratios of 3. Transmission electron microscopy indicated a polycrystalline structure with preferred orientation resulting from columnar grain growth. Individual grains had average diameters of 450 Å and consisted of microcrystallites with a typical size of 40 Å and tilt angles of $\sim 1^\circ$. The shortened electronic mean free path in such films ensures that the Ginzburg-Landau parameter is well within the type-II regime.⁶ The films were patterned using photolithography and Ar-ion milling into rings with outer and inner diameters of 98 and 15 μm , respectively. After patterning, a 8000-Å-thick coating of spin on glass was deposited, and served as a smooth, pinhole-free insulating substrate for subsequent fabrication of two Hall probes defined photolithographically from a 4000-Å-thick, thermally evaporated bismuth film. Each Hall probe measured the average perpendicular component of the field over its 3 $\mu\text{m} \times 5 \mu\text{m}$ active area, and was calibrated for both the Hall and the magnetoresistive response. One probe was positioned at the center of the ring’s hole (“hole probe”) and was used to monitor the *total* flux accumulating in the hole from motion anywhere on the ring. The other was 22 μm radially off center and directly above the ring (“ring probe”). It mea-

sured the local internal field, B , and thus the *local* vortex density. We were able to resolve changes of one superconducting flux quantum, ϕ_0 , or equivalently, a single vortex under the ring probe. For the hole probe, this translates to a resolution of about 10 vortices since flux spreads out uniformly within the hole.

The magnetic response of the rings were studied as a function of temperature, $1.4 \leq T \leq 10$ K, and magnetic field, $|H| < 4$ kG, applied perpendicular to the plane of the film. The temperature of the copper cold finger on which the samples were mounted was controlled to within ± 5 mK. Below, we describe in detail our findings for a typical sample as the applied field is slowly ramped up and down over the interval $-500 < H < 500$ G.¹¹ The four panels in Fig. 1 each show a single hysteresis loop, $B(H)$, characteristic of the distinct behavior we observe as part of a continuous evolution as the temperature is lowered. Except for Fig. 1(d), the ring-probe's trace is always nested within that of the hole probe, indicating a decreasing (on ramp up; or increasing on ramp down) radial flux density across the ring, as expected from the Bean model. When the flux density gradient exceeds the critical current, J_c , the driving force is large enough to depin vortices. Sudden changes in the flux density, resulting from avalanches, are detected as discrete jumps in B [see Figs. 1(b)–1(d)]. Not all avalanche events are spatially correlated for the two probes, indicating that both global and local readjustments of the internal magnetic profile may occur. Except for the regime corresponding to Fig. 1(c), avalanches occur randomly and successive hysteresis loops taken under identical conditions differ in the details of their structure. This explicitly demonstrates that the avalanches are not due to macroscopic inhomogeneities in the sample.

We accumulated statistics of the avalanche occurrences by repeatedly cycling around hysteresis loops. In Fig. 2 we plot the avalanche events observed over two cycles around the hysteresis loop at each temperature. Each symbol represents one avalanche of size, s , for the hole probe in Fig. 1.¹² As the temperature (or field, see below) is lowered from T_c , the distributions, $D(s)$, of avalanche sizes initially become broader. We also find that the shape of $D(s)$ changes. This is shown in the inset of Fig. 2. Here, variable width binning of the data is used to minimize statistical fluctuations without compromising resolution in s . Avalanche events were recorded over *many* hysteresis loops and then sorted by size and binned into groups of 25 consecutive sized events. The average event size was calculated for each group and all 25 events were placed into this one bin. Dividing by the range of avalanche sizes in each group gave $D(s)$.

For reduced temperatures $t \equiv T/T_c > 0.35$, flux jumps are rarely complete, i.e., they do not extend to the $B=H$ line, and are not narrowly distributed in size. Instead, $D(s)$ is relatively broad and was found to approximate the form,⁴ $D(s) \propto \exp(-s/s_0)$, over this temperature range. Fits to this form show that the mean avalanche size, s_0 , increases by nearly a factor of 5 as the temperature decreases from $t=0.5$ to 0.35. The dashed curve in Fig. 2 highlights this abrupt increase.

As t falls below 0.3, the system develops a clear deficiency of small- to intermediate-sized avalanches $s < 10^3$, and $D(s)$ shows a prominent peak around $s = 2000\phi_0$. This

maximum avalanche size is limited only by the maximum shielded or trapped field, which depends on sample size and critical current, $J_c(T, B)$. The magnetic response in this temperature range resembles a relaxation oscillator [Fig. 1(c)]. Note that the ring probe is always the first to sense the propagation of the flux front, which confirms that a flux gradient is repeatedly being established and destroyed across the ring. These large avalanches are most likely system spanning, eliminating any flux gradient between the two probes and resulting in a situation where, immediately after the avalanche, a significant fraction of the ring has magnetic induction *larger* than the applied field. The origin of these crossings of the $B=H$ line [see the dashed line in Fig. 1(c)] is poorly understood; we tentatively associate them with non-equilibrium thermal properties and demagnetization effects of our sample geometry.

At the lowest temperatures, $t < 0.2$ [Fig. 1(d)] $D(s)$ becomes broader again, but not of exponential form. Unlike the monotonic dependence of the radial flux density at higher t , the difference between applied field and magnetic induction can now be greater at the ring probe than at the hole probe. Also, avalanches now are triggered irrespective of the field profile near the center of the ring, occurring for both $B_{\text{ring}} < B_{\text{hole}}$ and $B_{\text{ring}} > B_{\text{hole}}$. Together, this is evidence that magnetic flux is entering inhomogeneously into the sample, perhaps as magnetic “fingers.”^{6,13}

We also explored the ramp rate dependence of the avalanche activity, which we found to remain unaffected for rates ranging over four decades from 2 mG/s to 20 G/s. This shows that the system is in the slowly driven regime, i.e., avalanche events do not overlap. Moreover, the occurrence of an avalanche depends only on the change in field after the previous avalanche and shows no correlation to the time passed after an avalanche. We were unable to determine the distribution of avalanche durations with our instrumentation, but an upper limit is 2 ms for the largest events. This is in accord with a simple estimate for the magnetic diffusivity, $D_m = \rho/\mu_0$, which yields avalanche durations, $\tau \sim r_0^2/D_m$, of microseconds or less for our samples. By comparison, the thermal diffusivity, $D_T = k/\gamma C$, is larger, and the Nb ring remains spatially isothermal, except for $t > 0.9$. Here, r_0 is the outer radius of the ring, γ is the density of Nb, and we used the Wiedemann-Franz law to calculate the thermal conductivity, k , and the tabulated temperature dependence for the specific heat, C , of bulk single-crystal Nb in the superconducting state.¹⁴ Thus, a flux jump corresponds to the case where rapid heating takes place on the background of a “frozen-in” spatial distribution of magnetic flux.

We now turn to a model for the thermal stability of the Bean state to magnetic flux jumps. We calculate the heat generated due to vortex motion, Q_{vm} , which is balanced against heat absorption by the ring, $\gamma C \Delta T$, and heat removal through the substrate, $C_h \Delta T$, where ΔT is the peak temperature rise during a flux jump. Over the course of a flux jump, $C_h \approx h\tau/d$, where d is the film thickness and $h = 300 \text{ T}^3 \text{ W m}^{-2} \text{ K}^{-1}$ is a temperature-dependent heat transfer coefficient typical of metal-sapphire interfaces.¹⁵ The ratio $Q_{\text{vm}}/(\gamma C + C_h)\Delta T$ defines a stability parameter β .¹⁶ The effectiveness of heat transfer in relation to specific heat as a stabilizing factor is contained in the denominator of this ratio. When $\beta > 1$ the Bean state is unstable, and the smallest

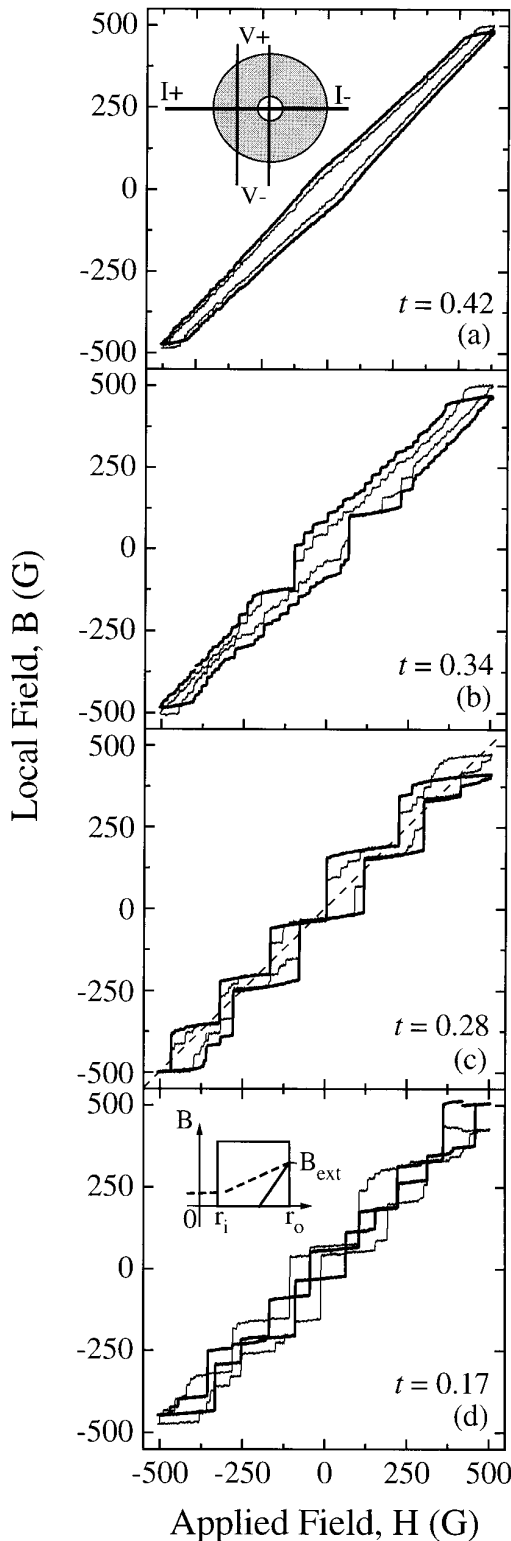


FIG. 1. Hysteresis loops, $B(H)$, taken at a field ramp rate of 0.25 G/s at various reduced temperatures, $t = T/T_c$, for the ring probe (thin line) and the hole probe (thick line). Predominantly smooth vortex motion at high t (a) is replaced by avalanche behavior at lower temperatures (b)–(d). The inset of (a) shows the sample's ring geometry and the positions of the gaussmeters. In (c), the magnetic response is reminiscent of a relaxation oscillator. Inset of (d): sketch of magnetic field profile in a cross-sectional view of the ring (see text). Solid lines (dashed lines) represent the profile immediately before (after) an avalanche.

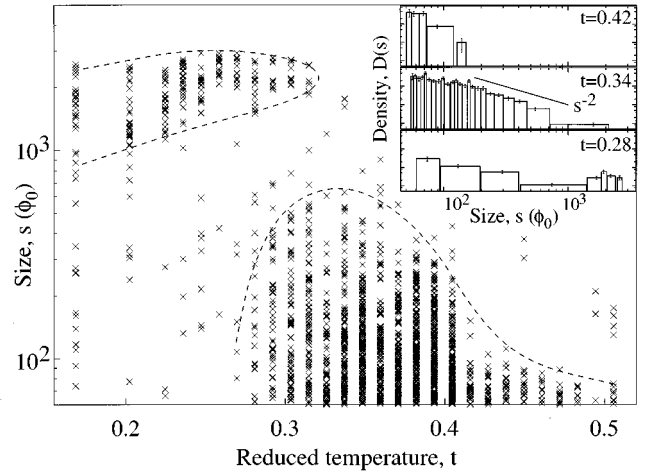


FIG. 2. Scatter plot of observed avalanches for the hole probe in Fig. 1 as a function of reduced temperature t . Each symbol represents one avalanche of size s . Data shown at each temperature are for two hysteresis loops. The dashed curves are guides to the eye, bounding size ranges of predominant event activity. An appreciable range of continuously distributed event sizes (1–2 decades) occurs only between $0.3 < t < 0.4$. The “island” with $s > 10^3$ corresponds to system-spanning avalanches. Inset: distribution of avalanche sizes, $D(s)$, for three temperatures corresponding to Figs. 1(a)–1(c). Vertical scale is logarithmic. Variable width binning (see text) is used to preserve resolution in s . The normalization is such that $D(s)ds$ is proportional to the average number of avalanches recorded with sizes between s and $s + ds$ per hysteresis loop.

perturbation, e.g., a temperature fluctuation, will initiate a flux jump. The size of the jump is related through $J_c(T, B)$ to the temperature at which heat from vortex motion is balanced by the heat capacity and cooling. For our ring geometry $\beta \equiv [\mu_0 J_c dr_0 / 5.1 \cdot (\gamma C + 130 T^3)] (-dJ_c / dT)$, where $C \sim T^3$ (mJ/mol K).¹⁴ In this expression, we have accounted for the fact that the field shielded at the center of a disc-shaped superconductor is $J_c d$, and not $J_c r_0$.¹⁷ We estimate β by calculating the temperature dependence of the critical current from the measured external magnetization envelope, $B-H = \mu_0 J_c d$. We find that $\beta > 1$ for $t < 0.37$, in good agreement with the rapid increase in avalanche size shown in Fig. 2. The close agreement with the model is perhaps fortuitous since important parameters, such as $C(T, H)$, $k(T)$, and $h(T)$ are difficult to measure and expected to depend strongly on the film's microstructure and impurities. Despite these shortfalls, however, the avalanche behavior over the entire H - T plane can be qualitatively accounted for by the model, as we outline below.

At high t , $\beta \ll 1$ and a large heat capacity serves to stabilize the Bean state. Thermal effects are negligible and the competition between vortex-vortex and vortex-defect interactions governs the nature of the motion. This regime corresponds to the hysteresis loops in Fig. 1(a) which are predominantly smooth and continuous. At first glance this constitutes a possible discrepancy with simulations³ and Lorentz microscopy⁷ of field-gradient-driven vortices in Nb films at comparably high temperatures which show individual vortices perform discrete hops. However, these hops are extremely fast and a recent analysis¹⁸ of Lorentz microscopy image sequences has shown directly that the resulting time-average flux motion is rather fluidlike.

At low t , the heat capacity of Nb is rapidly reduced and $\beta \gg 1$. Vortex motion can result in a significant local temperature rise which then propagates to surrounding areas, triggering further vortex motion. This positive feedback process, which essentially supplies “thermal inertia” to vortices, gives rise to global avalanches and inevitably results in a predominance of complete flux jumps of a characteristic size, see Fig. 1(c). One may invert the expression for the stability parameter β and arrive at a length scale $r(\beta=1)$ at which the first flux jump is to occur. When $r=r_0$, the Bean state becomes unstable. Shorter lengths at lower temperatures lead to instabilities of a thin edge layer where the flux gradient is first established, see inset of Fig. 1(d) and ring-probe data in Fig. 1(c). This precludes the formation of a Bean state across the entire sample and has important consequences for experiments which investigate the statistical properties of vortex avalanches about an assumed Bean state using global measuring techniques.^{4,5} Instabilities in this edge layer may result in the irregular magnetic profiles observed at the lowest temperatures. However, the inhomogeneous character of flux penetration is suggestive of a local mechanism. One possibility is that heat generated from flux moving along routes of weak pinning is rapidly removed through the substrate rather than initiating the propagation of a thermal quench front across the film, e.g., if the thermal conductivity of the superconductor is sufficiently reduced at low t .

The crossover temperatures between these dynamical regimes are field dependent, shifting to lower temperatures at higher fields. We have observed an evolution similar to Figs. 1 and 2, but as a function of field, by examining hysteresis loops extending to 3 kG at fixed low temperatures.¹⁹ Such a field dependence arises naturally within our model since $C(H,T)$ of a superconductor increases with H .²⁰

The simple thermal stability model leaves open a number of intriguing questions. In particular, while it can account for

a range of flux jump sizes, it cannot predict the shape of the size distribution. The broad distribution of avalanche sizes seen in previous experiments^{4,5} and that we observe over a narrow temperature interval $0.3 < t < 0.4$ may be associated with the regime where β is marginally greater than 1. In this case, an increase in the heat capacity brought on by the temperature rise from an avalanche event may lead to $\beta < 1$ (negative feedback), preventing further growth of the instability. Nevertheless, even in this regime, we find that the majority of flux jumps are spatially correlated between the Hall probes, which suggests that an avalanche is associated with a reduction of the flux gradient uniformly throughout the sample rather than affecting only local areas. This observation contrasts with SOC-based avalanche mechanisms, as does the finding that $D(s)$ approximates a power law, if at all, only over a very limited range (about one decade in s) and only after careful tuning of an external parameter (temperature in our case). Rather, our results appear similar to dynamical responses found in spring block models,²¹ “switching” charge density waves,²² or real sandpiles.²³ Moreover, our stability analysis indicates that, since β scales with r_0 (or r_0^2 in bulk samples), the system becomes less stable with increasing size. For sufficiently large r_0 , therefore, the typical response will consist of system-spanning breakdown events.

We thank B. Vuchic and K. Gray for assistance with sample preparation, R. Cook and M. Kirk for TEM analysis, and J. Fendrich, W. K. Kwok, and B. Glagola for the heavy-ion irradiation at the ATLAS source. This work was supported in part by the NSF through the Science and Technology Center for Superconductivity (DMR 91-20000) and the MRSEC (DMR-9400379) programs, and by the DOE, Basic Energy Sciences-Materials Science (No. W-31-109-ENG-38).

-
- ¹C. P. Bean, Phys. Rev. Lett. **8**, 250 (1962).
²P. Bak, C. Tang, and K. Wiesenfeld, Phys. Rev. A **38**, 364 (1988).
³O. Pla and F. Nori, Phys. Rev. Lett. **67**, 919 (1991); C. J. Olson, C. Reichhardt, J. Groth, S. Field, and F. Nori (unpublished).
⁴C. Heiden and G. I. Rochlin, Phys. Rev. Lett. **21**, 691 (1968).
⁵S. Field, J. Witt, and F. Nori, Phys. Rev. Lett. **74**, 1206 (1995).
⁶C. A. Duran *et al.*, Phys. Rev. B **52**, 75 (1995).
⁷K. Harada *et al.*, Nature **360**, 51 (1992).
⁸S. T. Stoddart *et al.*, Supercond. Sci. Tech. **8**, 459 (1995).
⁹R. G. Mints and A. L. Rakhmanov, Rev. Mod. Phys. **53**, 551 (1981); S. L. Wipf, Cryogenics **31**, 936 (1991), and references therein.
¹⁰R. J. Zieve *et al.*, Phys. Rev. B **53**, 11 849 (1996).
¹¹Similar behavior was found for samples irradiated with 1.1 GeV uranium atoms. Irradiation can create columnar defects in the high- T_c compounds; see R. Wheeler *et al.*, Appl. Phys. Lett. **63**, 1573 (1993). However, TEM studies found no evidence of irradiation-induced defects in Nb. The effect on the magnetic response was also found to be insignificant.
¹² $D(s)$ is ill defined for the ring probe which cannot measure avalanche sizes larger than its active area.
¹³P. Leiderer *et al.*, Phys. Rev. Lett. **71**, 2646 (1993).
¹⁴H. A. Leupold and H. A. Boorse, Phys. Rev. **134**, A1322 (1964).
¹⁵D. A. Neeper and J. R. Dillinger, Phys. Rev. **135**, A1028 (1964); W. J. Skocpol, M. R. Beasley, and M. Tinkham, J. Appl. Phys. **45**, 4064 (1974); K. E. Gray *et al.*, J. Phys. F **13**, 405 (1983).
¹⁶M. N. Wilson, *Superconducting Magnets* (Oxford University Press, New York, 1983).
¹⁷M. Däumling and D. C. Larbalestier, Phys. Rev. B **40**, 9350 (1989).
¹⁸C. H. Sow, A. Tonomura, G. Crabtree, and D. G. Grier (unpublished).
¹⁹E. R. Nowak *et al.* (unpublished).
²⁰Y. S. Touloukian and E. H. Buyco, *Thermophysical Properties of Matter* (Plenum, New York, 1970).
²¹M. de Sousa Vieira, G. L. Vasconcelos, and S. R. Nagel, Phys. Rev. E **47**, R2221 (1993); J. M. Carlson, J. S. Langer, and B. E. Shaw, Rev. Mod. Phys. **66**, 657 (1994).
²²J. Levy *et al.*, Phys. Rev. Lett. **68**, 2968 (1992); R. P. Hall, M. F. Hundley, and A. Zettl, Phys. Rev. B **38**, 13 002 (1988).
²³H. M. Jaeger and S. R. Nagel, Science **288**, 1523 (1992), and references therein.